frontiers in Molecular Neuroscience

BRIEF RESEARCH REPORT
published: 06 January 2022
doi: 10.3389/fnmol.2021.667143

A Versatile Clustered Regularly Interspaced Palindromic Repeats Toolbox to Study Neurological $Ca_V3.2$ Channelopathies by Promoter-Mediated Transcription Control

Despina Tsortouktzidis[1], Anna R. Tröscher[1,2], Herbert Schulz[3], Thoralf Opitz[4], Susanne Schoch[1], Albert J. Becker[1†] and Karen M. J. van Loo[1,5†]*

[1] Institute of Neuropathology, Medical Faculty, Section for Translational Epilepsy Research, University of Bonn, Bonn, Germany, [2] Department of Neurology, Kepler University Hospital, Johannes Kepler University Linz, Linz, Austria, [3] Department of Microgravity and Translational Regenerative Medicine, Clinic for Plastic, Aesthetic and Hand Surgery, Otto von Guericke University, Magdeburg, Germany, [4] Institute of Experimental Epileptology and Cognition Research, Medical Faculty, University of Bonn, Bonn, Germany, [5] Department of Epileptology and Neurology, RWTH Aachen University, Aachen, Germany

OPEN ACCESS

Edited by:
Felix Viana, Institute of Neurosciences, Spanish National Research Council (CSIC), Spain

Reviewed by:
Arnaud Monteil, Centre National de la Recherche Scientifique (CNRS), France
Luis Quintino, Lund University, Sweden

***Correspondence:**
Karen M. J. van Loo
kvanloo@ukaachen.de

† These authors have contributed equally to this work

Specialty section:
This article was submitted to Methods and Model Organisms, a section of the journal Frontiers in Molecular Neuroscience

Received: *12 February 2021*
Accepted: *15 December 2021*
Published: *06 January 2022*

Citation:
Tsortouktzidis D, Tröscher AR, Schulz H, Opitz T, Schoch S, Becker AJ and van Loo KMJ (2022) A Versatile Clustered Regularly Interspaced Palindromic Repeats Toolbox to Study Neurological $Ca_V3.2$ Channelopathies by Promoter-Mediated Transcription Control. Front. Mol. Neurosci. 14:667143. doi: 10.3389/fnmol.2021.667143

Precise genome editing in combination with viral delivery systems provides a valuable tool for neuroscience research. Traditionally, the role of genes in neuronal circuits has been addressed by overexpression or knock-out/knock-down systems. However, those techniques do not manipulate the endogenous loci and therefore have limitations. Those constraints include that many genes exhibit extensive alternative splicing, which can be regulated by neuronal activity. This complexity cannot be easily reproduced by overexpression of one protein variant. The CRISPR activation and interference/inhibition systems (CRISPRa/i) directed to promoter sequences can modulate the expression of selected target genes in a highly specific manner. This strategy could be particularly useful for the overexpression of large proteins and for alternatively spliced genes, e.g., for studying large ion channels known to be affected in ion channelopathies in a variety of neurological diseases. Here, we demonstrate the feasibility of a newly developed CRISPRa/i toolbox to manipulate the promoter activity of the *Cacna1h* gene. Impaired, function of the low-voltage-activated T-Type calcium channel $Ca_V3.2$ is involved in genetic/mutational as well as acquired/transcriptional channelopathies that emerge with epileptic seizures. We show CRISPR-induced activation and inhibition of the *Cacna1h* locus in NS20Y cells and primary cortical neurons, as well as activation in mouse organotypic slice cultures. In future applications, the system offers the intriguing perspective to study functional effects of gain-of-function or loss-of-function variations in the *Cacna1h* gene in more detail. A better understanding of $Ca_V3.2$ channelopathies might result in a major advancement in the pharmacotherapy of $Ca_V3.2$ channelopathy diseases.

Keywords: ion channelopathies, Cacna1h promoter modulation, CRISPR-induced activation, CRISPR-induced inhibition, T-Type calcium channel $Ca_V3.2$

INTRODUCTION

The human genome encodes approximately 400 ion channel genes, encompassing both voltage-gated and ligand-gated ion channels (Hutchings et al., 2019). Ion channels are pore forming membrane proteins that allow ionic flows across membranes and are crucial for normal functioning of many tissues, including the central and peripheral nervous system, heart, kidney, and liver (Cannon, 2007). Ion channel dysfunctions, also coined as ion "channelopathies," have been associated with a large variety of diseases. Besides disorders of the nervous system (e.g., epilepsy, ataxia, Alzheimer's disease, and Autism spectrum disorders), also cardiac arrhythmia and several muscle, endocrine, and renal disorders are linked to dysfunction of ion channels (Wang et al., 1996; Heeringa et al., 2009; Ryan et al., 2010). Still, many molecular and structural mechanisms of how channelopathies convert cells from a health to disease state are not fully understood, including critical time-windows during development as well as the potential reversibility by reconstituting normal expression/function of affected molecules. Major obstacles to manipulate ion channels are given by their large size, which limits options for widespread and *in vivo* overexpression and their diversification by alternative splicing.

Genetic editing using a modified CRISPR (clustered regularly interspaced palindromic repeats) system could be a powerful approach for the manipulation of large proteins that cannot be done by conventional techniques. Recently, substantial progress has been made in genomic editing by using specific applications of the CRISPR technique, including the CRISPR *activation* (CRISPRa) and CRISPR *interference/inhibition* (CRISPRi) technology. CRISPRa uses a catalytically dead Cas9 (dCas9) enzyme fused with a highly efficient transcriptional activator complex consisting of the tripartite transcriptional activator VP64-p65-Rta (VPR), shown to increase target gene expression even up to 320-fold (Chavez et al., 2015). CRISPRi also uses the dCas9 enzyme and is fused with the transcriptional repressor KRAB (Krüppel-associated box) protein, which results in up to 60–80% reduction in the expression of endogenous eukaryotic genes (Gilbert et al., 2013). Using these enhanced CRISPR technology systems, the expression of genes can be modified in their native context with utmost precision. Therefore, this strategy will be particularly useful for (a) the overexpression of large proteins, which is difficult to accomplish by conventional techniques and (b) for alternatively spliced genes.

In this study, we have developed a CRISPRa/i toolbox for manipulating the expression of a well-described ion channelopathy gene, *Cacna1h,* encoding the low-voltage-activated T-Type calcium channel $Ca_V3.2$. Ion channelopathies for *Cacna1h* have been described particularly for epilepsy variants (Khosravani et al., 2004, 2005; Powell et al., 2009; Souza et al., 2019), but were also reported for other neurological diseases including autism spectrum disorders (Splawski et al., 2006), amyotrophy lateral sclerosis (ALS; Rzhepetskyy et al., 2016) and pain disorders (Souza et al., 2016). By using the unique CRISPRa/i toolbox, we demonstrate to specifically modulate *Cacna1h* gene expression in different cell types in order to closely recapitulate $Ca_V3.2$ channelopathies.

MATERIALS AND METHODS

Design of sgRNAs

sgRNA design was performed using the computational software Benchling (Cloud-Based Informatics Platform for Life Sciences R&D | Benchling, 2021). The previously validated *Cacna1h* promoter (Van Loo et al., 2012) was used to set the sgRNAs targeting sequence. The sgRNAs were selected based on their local off-target scores, proximity to the start-ATG, a distance of at least 50 bp between each other and a 100% match in targeting both the mouse and rat genome.

Cloning

All primer sequences used for cloning are shown in **Supplementary Table 1**. As a basis for our cloning strategies, we exchanged the hybrid cytomegalovirus-actin-globin promoter of pAAV-MCS (Agilent) by the human synapsin (hSyn) promoter (Kügler et al., 2003) using the *Mlu*I/*Bsu*15I restriction sites. In order to generate the pAAV-U6-sgRNA plasmids, we cloned a U6-*Bbs*I/*Bbs*I cassette into the pAAV-hSyn-MCS backbone. For this, the U6-*Bbs*I/*Bbs*I cassette was PCR-amplified from px458 [Addgene #48138, Ran et al. (2013)] and inserted by in-fusion cloning (IFC; Takara Bio Europe/Clontech) into *Mlu*I/*Asi*SI-digested pAAV-hSyn-MCS. Next, the polyA was removed by digestion with *Afe*I/*Pml*I and subsequent self-ligation. Finally, the sgRNAs were annealed and cloned into the *Bbs*I sites (Cloud-Based Informatics Platform for Life Sciences R&D | Benchling, 2021). Briefly, the annealing was performed using 10 μM of each oligo, 1X T4 ligation buffer and 5U of T4 PNK in a total volume of 10 μL, following an incubation at 37°C for 30 min and 95°C for 5 min, the reaction was cooled at room temperature. The annealed oligos (1 μL) were cloned using 25 ng of construct, 1X T4 ligation buffer, T4 ligase (200 U) and *Bbs*I (2.5 U) in a total volume of 10 μL, the reaction was performed by 30 cycles at 37°C for 5 min and 23°C for 5 min.

The all-in-one CRISPRa lentiviral system was generated by replacing the promoter of pLenti-Ef1a-dCas9-VPR [Addgene#114195, Savell et al. (2019)] by the hSyn promoter using IFC. For this, pAAV-hSyn-MCS was used as PCR template for the hSyn promoter and cloned into *Afe*I/*Kpn*I-digested pLenti-Ef1a-dCas9-VPR. In a second step, the *Cacna1h* and *LacZ* sgRNA sequences from the pAAV-U6-sgRNA plasmids (see above) were cloned by IFC into the *Pac*I site of pLenti-syn-dCas9-VPR, resulting in pLenti-U6-sgRNA$_{(Cacna1h/LacZ)}$-Syn-dCas9-VPR.

The all-in-one CRISPRi lentiviral system was produced by replacing the hU6-sgRNA-hUbC cassette of pLenti-hU6-sgRNA-hUbC-dCas9-KRAB-T2a-eGFP [Addgene#71237, Thakore et al. (2015)] for the hSyn promoter by IFC. The backbone was digested with *Xba*I/*Pac*I and the hSyn promoter PCR amplified from pAAV-hSyn-MCS, resulting in pLenti-hSyn-dCas9-KRAB-T2A-eGFP. Subsequently, the U6-sgRNA$_{Cacna1h/LacZ}$ cassettes from the pAAV-U6-sgRNA plasmids (see above) were inserted into the *Pac*I site of pLenti-hSyn-dCas9-KRAB-T2A-eGFP by IFC.

pTRE-dCas9-VPR was generated by replacing the promoter of pLenti-Ef1a-dCas9-VPR [Addgene#114195, Savell et al. (2019)] for the tetracycline response element (TRE) of the pK031.TRE-Cre [Addgene#69136 (Mizuno et al., 2014)] by IFC using the *Afe*I/*Kpn*I restriction sites. pTRE-dCas9-KRAB-T2A-eGFP was produced by replacing the promoter of the previously generated pLenti-hSyn-dCas9-KRAB-T2A-eGFP with the TRE of pK031.TRE-Cre [Addgene#69136 (Mizuno et al., 2014)] by IFC, using the *Pac*I/*Xba*I restriction sites. pAAV-hSyn-rtTA was generated by IFC using *Eco*RI/*Sal*I-digested pAAV-hSyn-MCS and the rtTA sequence PCR-amplified from mCreb1 in pInducer20, kindly provided by Dasgupta and co-workers (Chhipa et al., 2018).

Cell Culture, Transfection, and Luciferase Assay

NS20Y cells (Sigma, #08062517) were maintained at 37°C and 5% CO_2 in DMEM (Sigma, D6546) supplemented with 10% (v/v) heat inactivated FBS, 2 mM L-Glutamine, 100 units/mL penicillin/streptomycin. Cells were transfected in 24 well plates using Lipofectamine (Invitrogen) following the manufacturer's instructions. The DNA concentration used per well: *Cacna1h*-Luciferase or *Cacna1h*-mRuby 100 ng, CMV-VPR [Addgene# 63798, (Chavez et al., 2015)] or CMV-KRAB [Addgene#110821, (Yeo et al., 2018)] 200 ng, pAAV-sgRNA 200 ng and hypB-CAG-2A-eGFP 100 ng. Following 48 h after transfection, the cells were imaged or collected for luciferase assays. Luciferase assays were performed using the Dual Luciferase Reporter Assay System (Promega) according to the manufacturer's specifications. Firefly luciferase activity was determined using the Glomax Luminometer (Promega).

Viral Production and Neuronal Transduction

AAV1/2 viruses were produced by large-scale triple $CaPO_4$ transfection of HEK293-AAV cells (Agilent, #240073) as described previously (Van Loo et al., 2012). Lentiviruses were produced in HEK293T cells using a second-generation lentiviral packaging system. The procedure was performed as described before (Van Loo et al., 2019). Dissociated primary neurons were prepared from mouse cortex (C57Bl6/N) at embryonic day 15–19 as described before (Woitecki et al., 2016). All animals were handled according to government regulations as approved by local authorities (LANUV Recklinghausen). All procedures were planned and performed in accordance with the guidelines of the University Hospital Bonn Animal-Care-Committee as well as the guidelines approved by the European Directive (2010/63/EU) on the protection of animals used for experimental purposes. Cells were kept in BME medium (Gibco) supplemented with 1% FBS, 0.5 mM L-glutamine, 0.5% glucose and 1X B27 at 37°C and 5% CO_2. Neuronal transduction was performed at days *in vitro* (DIV) 4 in 24 well plates containing 70,000 cells/well with a multiplicity of infection (MOI) of approximately 14. Cells were collected on DIV15 in lysis/binding buffer (Invitrogen, A33562) and stored at −80°C until mRNA extraction or at DIV20 for Western blot.

RNA Isolation and Real Time RT-PCR

RNA isolation and cDNA production was performed using Dynabeads mRNA Direct Micro Kit (Invitrogen, 61021) and RevertAid H Minus First strand cDNA Synthesis Kit (Thermo Fisher Scientific, K1632) following the manufacturer's instructions. Quantitative PCR was performed in a Thermal Cycler (BioRad C1000 Touch, CFX384 Real-Time system). The reaction was performed using 1X Maxima SYBR Green/Rox qPCR Master Mix (Thermo Fisher Scientific, K0223), 0.3 μM of each primer (for primer sequences see **Supplementary Table 2**) and 1/10 synthesized cDNA (for NS20Y and 1/2 for Neurons) for a total volume of 6.25 μL. The qPCR conditions were as follow: 2 min at 50°C, 10 min at 95°C, 40 cycles of 15 s at 95°C and 1 min at 59°C. mRNA quantification was performed by real-time RT-PCR using the ΔΔCt-method. Quantification was based on synaptophysin (Chen et al., 2001).

Protein Extraction and Western Blotting

Transduced cortical neurons (4,20,000 cells) were lysed in RIPA buffer (150 mM sodium chloride, 1% NP40, 0.5% sodium deoxycholate, 0.1% SDS, 50 mM Tris–HCl, pH8, protease inhibitor 1X, and phosphatase inhibitor 1X), loaded on 8% SDS polyacrylamide gels and transferred onto nitrocellulose membranes. Blots were blocked in 5% milk for 1 h and incubated overnight with a primary antibody against $Ca_V3.2$ (1:200, Sigma C1868). Following washing steps in PBS-T (0.1% Tween) the membrane was incubated with IRDye800 Goat anti-Rabbit (1:10,000, LI-COR Biosciences) for 45 min, washed and imaged. The membrane was subsequently incubated with anti-Tubulin antibody (1:5,000, ab6160) for 2 h at RT, washed and incubated with IRDye680 Goat anti-Rat (1:10,000, LI-COR Biosciences). Bands were detected with infrared Odyssey system (LI-COR Biosciences) and quantified using the software Image Studio Lite.

Mouse Organotypic Slices

Organotypic hippocampal slices were prepared from mice (C57Bl6/N) at postnatal day 3–6 as described before (Biermann et al., 2014). In brief, the hippocampus was isolated and cut in 350 μM thickness using a McIllwain tissue chopper. The slices were cultured in 6 well plates containing cell culture inserts 0.4 μM, 30 mm (Millipore) and medium (50% Neurobasal medium, 25% Hank's balanced salt solution (without $MgCl_2$, without $CaCl_2$), 25% horse serum, 0.65% D(+)-glucose, 0.01 M Hepes, 2 mM L-glutamine and 0.5X B27). Cultured slices were kept at 37°C, 5% CO_2.

Cell Imaging

Images were obtained using an inverted phase contrast fluorescent microscope (Zeiss Axio Observer A1 with objectives 20X, LD A-Plan and 5X, Fluar) and processed using Fiji. The cell surface area, set by the GFP fluorescence, was determined using the Weka trainable segmentation plugging. The integrated density, determined by the mRuby fluorescence was normalized to the cell surface area to obtain the reported values of integrated density/cell surface (IntDE/cell surfase).

Statistical Analyses

Statistical analyses were performed using GaphPad software. One sample *t*-test, Student *t*-test, and two way ANOVA followed by multiple comparison tests were used to compare significance of the results. Values were considered significant a $p < 0.05$. For all graphs data are displayed as mean ± SEM.

RESULTS

To modulate the promoter activity of the *Cacna1h* gene, we first designed sgRNAs sequences targeting the mouse and rat *Cacna1h* gene. Using the Benchling computational tool, we selected two sgRNAs binding 66 (sgRNA1) and 131 (sgRNA2) base pairs (bp) upstream of the start-ATG of the *Cacna1h* gene (**Figure 1A**). Next, we tested the efficiency of the two sgRNAs to target the *Cacna1h* promoter and regulate its activity in neuroblastoma NS20Y cells. For this, we transfected the two sgRNAs together with (i) a minimal reporter unit expressing mRuby under control of the rat *Cacna1h* promoter, (ii) a ubiquitous promoter expressing eGFP, and (iii) either a CRISPRa construct [dCas9-VPR, Chavez et al. (2015)] or a CRISPRi construct [dCas9-KRAB, (Yeo et al., 2018)] in NS20Y cells and analyzed the fluorescence intensity 2 days after transfection (**Figures 1B,C**). A strong activation of the *Cacna1h* promoter was observed after co-transfection with the CRISPRa construct and an inhibition after co-transfection with the CRISPRi construct (**Figure 1C**). No modulation was observed for the ubiquitous CAG-eGFP construct, indicating that the sgRNAs only affected the activity of the *Cacna1h* promoter (**Figure 1C**).

Next, we compared the modulatory effects of the two sgRNAs in both the CRISPRa and CRISPRi systems. A significant increase in *Cacna1h*-mRuby fluorescence activity was observed for the two single sgRNAs in the CRISPRa system (mean ± SEM = sgRNA1: 3.41 ± 0.26-fold increase, $p = 0.0026$; sgRNA2: 2.93 ± 0.16-fold increase, $p = 0.0012$), and reached similar levels as observed for the combination of the two sgRNAs (**Figure 1D**, left panel; mean ± SEM = sgRNA1 + 2: 3.60 ± 0.51-fold increase, $p = 0.015$). Also for the CRISPRi system, comparable modulatory effects were observed for sgRNA1 (mean ± SEM = 0.52 ± 0.078-fold decrease, $p = 0.0088$), sgRNA2 (0.51 ± 0.046-fold decrease, $p = 0.0017$) and the combination of the two sgRNAs (0.52 ± 0.10-fold decrease, $p = 0.017$; **Figure 1D**, middle panel). A control sgRNA targeting *Lac*Z did not have an effect on *Cacna1h* fluorescence intensity in the CRISPRa or CRISPRi system (**Figure 1D**, right panel), indicating that the modulatory effects observed for the two *Cacna1h*-sgRNAs were highly specific.

To confirm and precisely quantify the *Cacna1h*-specific CRISPRa and CRISPRi regulation, we next exchanged the mRuby reporter for a luciferase reporter gene (**Figure 1E**, left panel). As expected, transfection of the CRISPRa and CRISPRi components into NS20Y cells, resulted in an increase of luciferase activity for the CRISPRa system (**Figure 1E**, middle panel; sgRNA1: 5.44 ± 0.84-fold increase, $p = 0.034$; sgRNA2: 4.79 ± 0.80-fold increase, $p = 0.042$; sgRNA1 + 2: 6.75 ± 0.45-fold increase, $p = 0.006$) and a decrease for the CRISPRi system (**Figure 1E**, right panel; sgRNA1: 0.26 ± 0.087-fold decrease, $p = 0.013$; sgRNA2: 0.24 ± 0.039-fold decrease, $p = 0.0026$; sgRNA1 + 2: 0.12 ± 0.014-fold decrease, $p = 0.0003$). Also here, no significant differences were observed between the two sgRNAs or the combination of the two sgRNAs.

We next examined the endogenous *Cacna1h* mRNA expression levels after manipulation with the CRISPRa and CRISPRi systems using quantitative real-time RT-PCR. Since both sgRNAs showed similar effects on the *Cacna1h* reporter constructs (**Figures 1D,E**) we decided to use the combination of the two sgRNAs for this experiment. Activation of the system in NS20Y cells, resulted in augmentation of endogenous *Cacna1h* mRNA expression levels, whereas inhibition significantly decreased the *Cacna1h* mRNA expression levels (**Figure 1F**, right panel; CRISPRa: 2.69 ± 0.33-fold increase, $p = 0.036$; CRISPRi: 0.69 ± 0.018-fold decrease, $p = 0.0034$). No changes in *Cacna1h* expression were observed for the CRISPRa and CRISPRi controls (no sgRNA; **Figure 1F**, left panel). Altogether, these results confirmed that the present *Cacna1h*-CRISPR modulatory toolbox successfully can activate or inhibit endogenous *Cacna1h* expression in NS20Y cells.

We then probed whether the modulatory effects observed in NS20Y cells could also be observed in primary cultured neurons. For this, we transduced primary mouse cortical neurons at DIV4 with all-in-one CRISPRa/i lentiviruses (**Figure 2A**) and measured endogenous *Cacna1h* mRNA expression levels at DIV15 and protein levels at DIV20. Since the two sgRNAs displayed similar effects in NS20Y cells (**Figures 1D,E**), we decided to proceed with only one sgRNA (sgRNA2) to minimize unspecific effects in the neuronal cultures. Intriguingly, a strong activation was observed after transduction with CRISPRa lentiviruses both at the mRNA (**Figure 2B**, left panel, 4.37 ± 0.37-fold increase, $p = 0.0016$) and at the protein level (**Figure 2C**, 2.18 ± 0.42-fold increase, $p = 0.0046$). In addition, also inhibition of the system using CRISPRi in neuronal cultures resulted in a reduced *Cacna1h* expression at the mRNA (**Figure 2B**, right panel, 0.12 ± 0.049-fold change, $p = 0.032$) as well as at the protein level (**Figure 2D**, 0.39 ± 0.14-fold change, $p = 0.042$), indicating that sgRNA2 can efficiently modulate *Cacna1h* promoter activity in primary neurons. Although we observed additional non-specific bands in our Western blot experiments (**Supplementary Figure 1**), only the band of approximately 260 kDa corresponding to $Ca_V3.2$ increases or decreases in intensity after treatment with *Cacna1h*-CRISPRa and *Cacna1h*-CRISPRi, respectively.

To prove unequivocally that the *Cacna1h*-CRISPRa/i toolbox is specific for *Cacna1h* modulation, we next examined the mRNA expression levels of other calcium channel family members (*Cacna1g*, *Cacna1i,* and *Cacna1e*) after *Cacna1h*-CRISPRa/i targeting using quantitative real-time RT-PCR. No alterations were observed for any of the other calcium channels tested (**Figure 2E**), indicating that our newly developed *Cacna1h*-CRISPRa/i toolbox is highly specific for *Cacna1h* modulation.

In order to test if our system has the potential to be delivered in neuronal network structures *in vivo* we infected mouse organoptypic hippocampal slices with recombinant adeno-associated (rAAV) and lentiviruses encoding our *Cacna1h*-CRISPRa toolbox and a fluorescent reporter. After

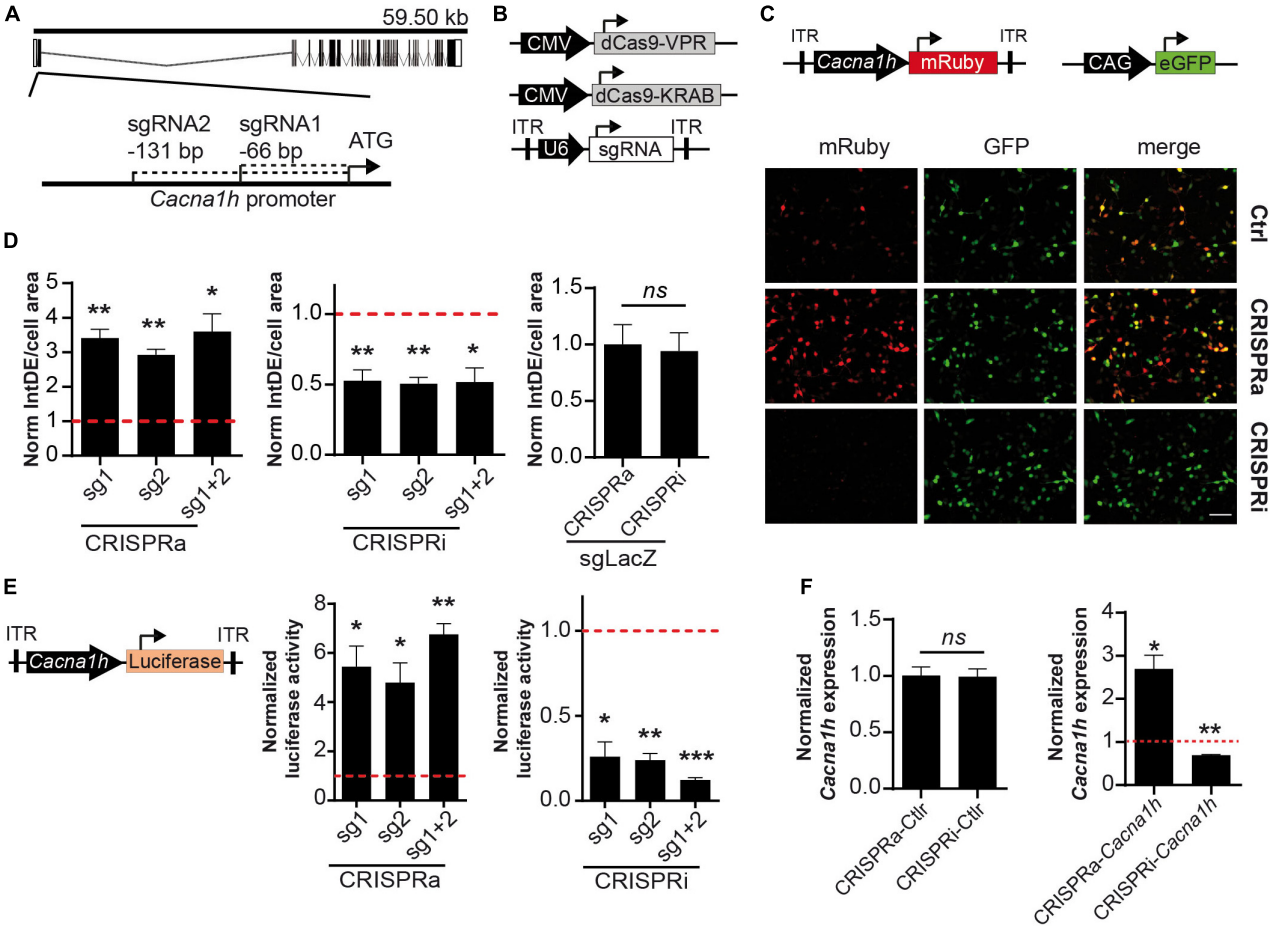

FIGURE 1 | Validation of the CRISPRa/i system for modulating *Cacna1h* expression. **(A)** Schematic representation of the *Cacna1h* mouse gene. Exons and introns are shown as boxes and dash lines, respectively. The position of sgRNA1 and sgRNA2 are indicated respective to the start-ATG (bp: base pairs). **(B)** Schematic illustration of the CRISPRa (CMV-dCas9-VPR), CRISPRi (CMV-dCas9-KRAB), and the sgRNA (pAAV-U6-sgRNA) constructs. **(C)** NS20Y co-transfected with CRISPRa or CRISPRi, the two sgRNAs targeting *Cacna1h* (or *LacZ* as control), the reporter pAAV-*Cacna1h*-mRuby, and a CAG-eGFP construct as internal control for transfection. Scale bar = 100 μm. **(D)** Quantification of integrated density (IntDE) of mRuby per cell surface area (defined by CAG-eGFP positive cells). Values of IntDE/cell area were normalized to the controls of each treatment: CRSIPRa-*LacZ* for CRISPRa and CRISPRi-*LacZ* for CRISPRi (One sample *t*-test, $N = 4$), $^*p \leq 0.05$, $^{**}p \leq 0.01$. **(E)** Luciferase activity of cells co-transfected with pAAV-*Cacna1h*-luciferase, CRISPRa or CRISPRi and sgRNAs targeting *Cacna1h* (or *LacZ* as control). Data normalized to each control: CRISPRa-*LacZ* for CRISPRa treatment and CRISPRi-*LacZ* for CRISPRi treatment (One sample *t*-test, $N = 3$), $^*p \leq 0.05$, $^{**}p \leq 0.01$, $^{***}p \leq 0.001$. **(F)** *Cacna1h* mRNA expression in NS20Y cells co-transfected with CRISPRa or CRISPRi. Left panel: Cells transfected with CRISPRa and CRISPRi without sgRNAs ($N = 3$, *t*-test). Right panel: *Cacna1h* mRNA expression levels in NS20Y cells transfected with CRISPRa or CRISPRi and sgRNAs targeting *Cacna1h* (sgRNA1 + 2). Values were normalized to the mean of CRISPRa and CRISPRi controls (lacking sgRNA) (One sample *t*-test, $N = 3$), $^*p \leq 0.05$, $^{**}p \leq 0.01$.

co-transduction with AAV-sgRNA, lenti-EF1a-dCas9-VPR (Savell et al., 2019) and the reporter AAV-*Cacna1h*-mRuby we observed a stronger signal of the red fluorescent protein when using the sgRNA targeting *Cacna1h* than in the control indicating an activation of the *Cacna1h* promoter *in vivo* (**Figure 2F**).

The *Cacna1h*-CRISPR toolbox we describe here was made for constitutive activation or inhibition of the *Cacna1h* transcripts. We next adapted the system for induced gene expression control by incorporating doxycycline-controlled Tet-On gene expression systems (Colasante et al., 2019; Zhang et al., 2019). In this way, *Cacna1h* expression can be activated or inhibited at a precise temporal resolution. We tested the system in primary cortical neurons with a combination of viruses that allow doxycycline-inducible CRISPR-*Cacna1h* activation (denoted as TET-ON-CRISPRa-*Cacna1h*; **Figure 3A**) or doxycycline-inducible CRISPR-*Cacna1h* inhibition (denoted as TET-ON-CRISPRi-*Cacna1h*; **Figure 3B**). Doxycycline was administered 4 days after viral transduction and mRNA was analyzed at DIV15. Interestingly, we observed an increase in *Cacna1h* expression after transduction with the TET-ON-CRISPRa-*Cacna1h* system following doxycycline treatment (**Figure 3C**; 1.85 ± 0.12-fold change, $p = 0.0015$), and a decrease in *Cacna1h* expression after TET-ON-CRISPRi-*Cacna1h* transduction and doxycycline treatment (**Figure 3D**; 0.28 ± 0.11-fold change, $p = 0.027$). No effect on *Cacna1h* expression was observed when using a control sgRNA targeting *LacZ* (**Supplementary Figure 2**). We thus present a proof of principle that *Cacna1h* expression can be activated or inhibited at a precise temporal resolution.

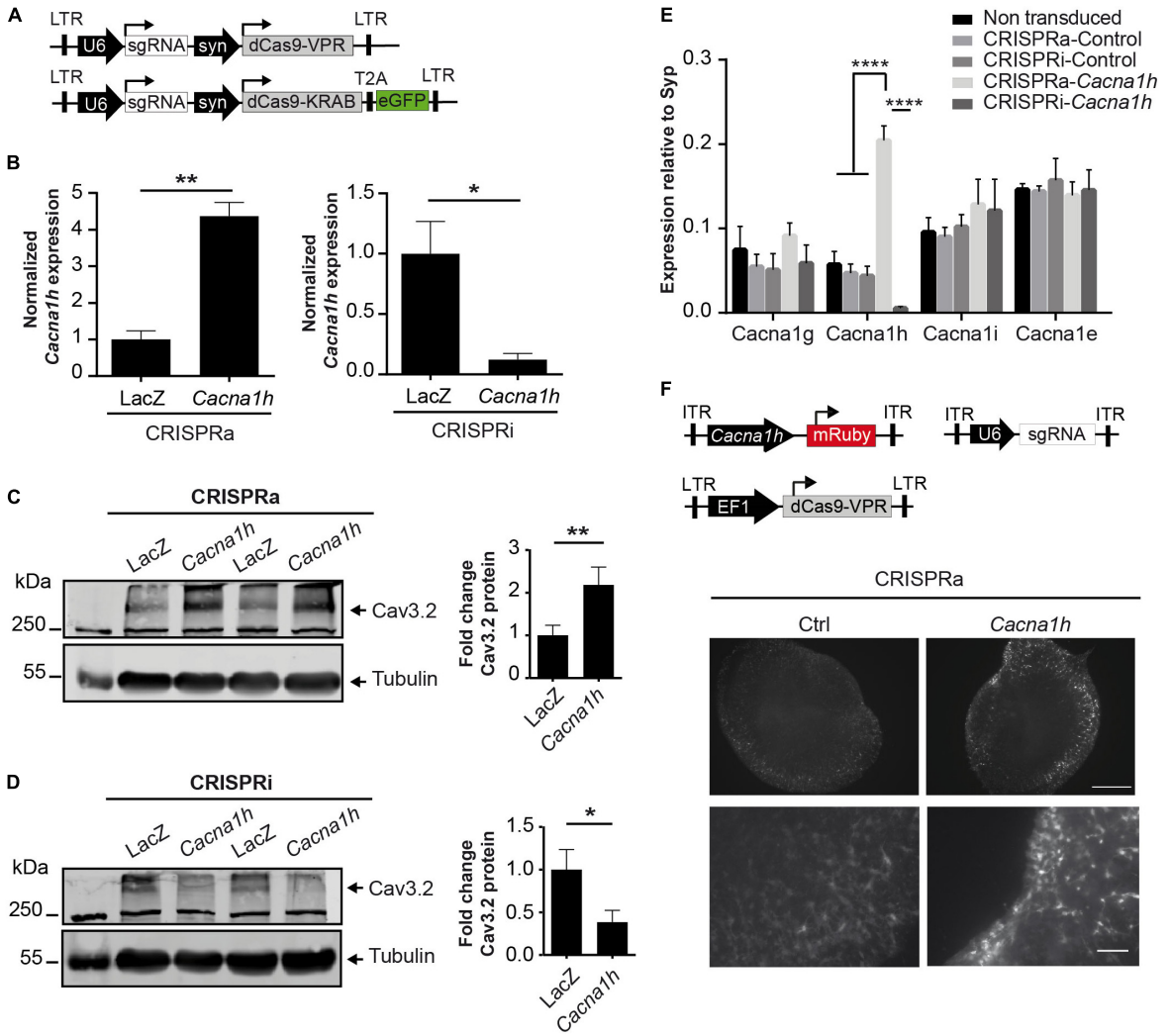

FIGURE 2 | CRISPRa/i modulates the endogenous expression of *Cacna1h* in primary neurons. **(A)** Schematic representation of the all-in-one lentiviral constructs for CRISPRa (Lenti-U6-sgRNA-syn-dCas9-VPR) and CRISPRi (Lenti-U6-sgRNA-syn-dCas9-KRAB-EGFP). **(B)** mRNA expression of *Cacna1h* in cultured neurons after transduction with the all-in-one lentivirus targeting either *Cacna1h* or the control (*LacZ*). Expression levels of *Cacna1h* relative to Synaptophysin in every treatment were normalized to the controls (CRISPRa-*LacZ* and CRISPRi-*LacZ*), $N = 3$, unpaired *t*-test, $^{*}p \leq 0.05$, $^{**}p \leq 0.01$. **(C)** Representative western blot and quantification of Cav3.2 protein levels in cortical neurons transduced with the all in one lentivirus for CRISPRa-*Cacna1h* (or *LacZ*, as control) ($N = 6$, paired *t*-test), $^{**}p \leq 0.01$. **(D)** Representative western blot and quantification of Cav3.2 protein levels in cortical neurons transduced with the all in one lentivirus for CRISPRi-*Cacna1h* (or *LacZ*, as control) ($N = 5$, paired *t*-test), $^{*}p \leq 0.05$. **(C,D)** Tubulin was used as loading control. Values of Cav3.2/Tubulin were normalized to the controls of each treatment: CRSIPRa-*LacZ* for CRISPRa and CRISPRi-*LacZ* for CRISPRi. **(E)** mRNA expression of different calcium channels in neurons transduced with the all-in-one lentiviral constructs targeting *Cacna1h*. Expression relative to synaptophysin ($N = 3$, Two way ANOVA, Tukey's multiple comparison test, $^{****}p \leq 0.0001$). **(F)** Mouse organotypic hippocampal slices transduced with the CRISPRa lentivirus, the AAV-U6-sgRNA and the reporter AAV-*Cacna1h*-mRuby (Scale bar of 500 μM for upper and 100 μM for lower panel).

DISCUSSION

Detailed analyses of the dynamic contribution of individual ion channels in the context of neuronal network function remains challenging, particularly in the context of mutational and transcriptional "channelopathies," in which for example the fine-tuned regulation of mRNA expression levels of affected genes, including *Cacna1h* plays a major role. Traditionally, the functional characterization of individual ion channels in terms of gain- and loss-of-function approaches has been addressed by the exogenous overexpression of genetically encoded proteins and by knock-down systems *via* RNA interference (RNAi)/genetic gene ablation (knock-out), respectively. Although very valuable, the applicability of these techniques has limitations (Kampmann, 2018).

Here, we present a modular method using a CRISPRa/i system that allows to manipulate the endogenous expression of *Cacna1h in vitro* and *in vivo*. This CRISPRa/i system applies specific sgRNAs directed to the *Cacna1h* promoter and a dCas9 fused to the transcriptional activator VPR or the transcriptional

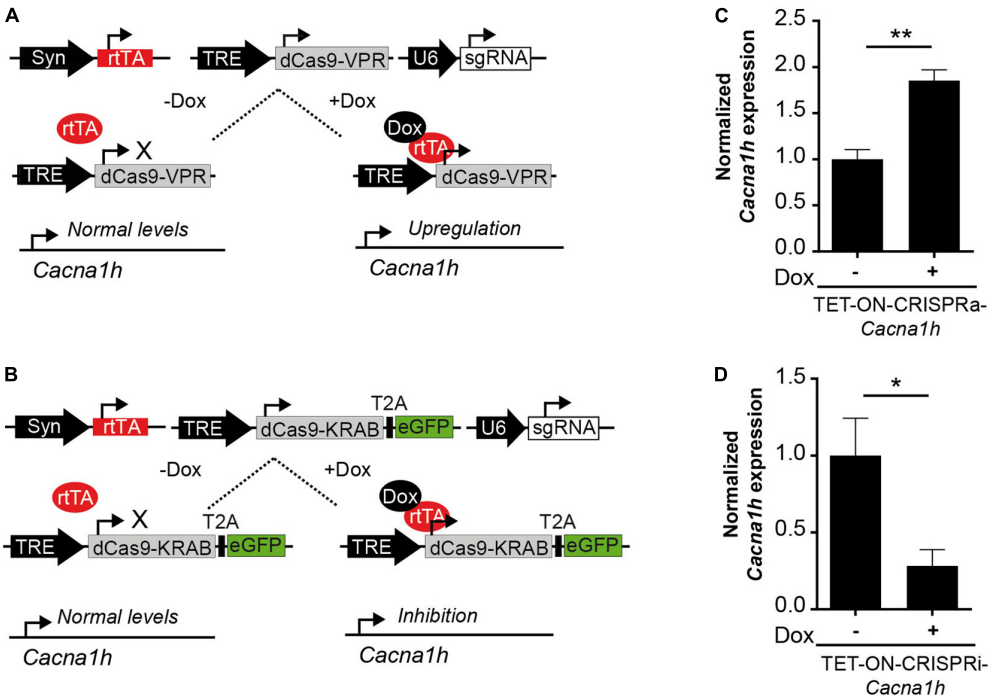

FIGURE 3 | Future perspectives to study *Cacna1h*-channelopathies. **(A)** Schematic representation of a TET-ON system for the conditional expression of CRISPRa (TRE-dCas9-VPR). Only in the presence of doxycycline (Dox) the reverse tetracycline-controlled transactivator (rtTA) binds to the tetracycline response element (TRE) inducing the expression of *Cacna1h*-CRISPRa resulting in augmented endogenous *Cacna1h* expression. **(B)** Schematic representation of a TET-ON system for the conditional expression of CRISPRi (TRE-dCas9-KRAB). Only in the presence of Dox, endogenous *Cacna1h* expression is inhibited. **(C)** *Cacna1h* mRNA expression levels of cultured neurons after transduction with the TET-ON-CRISPRa-*Cacna1h* system (pTRE-dCas9-VPR, pAAV-hSyn-rtTA and pAAV-sgRNA-*Cacna1h*) in the presence or absence of doxycycline (1 μg/mL) ($N = 4$, *t*-test), $^{**}p \leq 0.01$. **(D)** *Cacna1h* mRNA expression of cultured neurons after transduction with the TET-ON-CRISPRi-*Cacna1h* system (pTRE-KRAB-T2A-eGFP, pAAV-hSyn-rtTA, and pAAV-sgRNA-*Cacna1h*) in the presence or absence of doxycycline (1 μg/mL) ($N = 5$, *t*-test), $^{*}p \leq 0.05$.

inhibitor KRAB (Gilbert et al., 2013; Chavez et al., 2015) to induce changes in the endogenous expression of the *Cacna1h* gene. We provide evidence that both the CRISPRa and CRISPRi systems can specifically manipulate the endogenous expression of *Cacna1h* in dividing cells as well as in primary neuronal cultures. In addition, we demonstrate the possibility to activate the *Cacna1h* promoter in mouse organotypic hippocampal slices. Interestingly, the fold-change induction by CRISPRa occurred within a range also observed for $Ca_V3.2$ channelopathies (Becker et al., 2008), making our *Cacna1h*-CRISPR system highly suitable for analyzing this particular and also other channelopathies at the functional level.

Increasing the gene expression levels of *Cacna1h* in a high percentage of cultured cells, which is required for many downstream analyses, or *in vivo* requires the application of viral transduction systems. Here, our *Cacna1h*-CRISPRa toolbox has a clear advantage over conventional virally mediated overexpression approaches, where the limiting packaging capacity of the commonly used and easily applicable recombinant adeno-associated- and lenti-viruses, excludes the possibility to overexpress large proteins like *Cacna1h*. On the other hand, recombinant viruses with a higher packaging capacity, like Adeno- and Herpes Simplex virus, cannot be easily generated in the lab and are expensive to purchase. Since augmentation of proteins using the CRISPRa system is independent of their transcript size, even the large *Cacna1h* gene (mRNA transcript length up to 8.2 Kb) can be easily augmented using rAAV and lentiviruses, which can be produced in most molecular biology labs. Another advantage of the *Cacna1h*-CRISPRa system over conventional gain-of-function approaches is the endogenous modulation of the *Cacna1h* genomic locus, providing the opportunity to study the effects of abundant alternative splicing variants of *Cacna1h*. For *Cacna1h*, at least 12–14 alternative splicing sites have been described, resulting in the possibility to generate more than 4,000 alternative *Cacna1h* transcripts (Zhong et al., 2006). Such a complexity cannot be achieved by conventional overexpression of only one variant of *Cacna1h*. Also in terms of loss-of-function approaches, our *Cacna1h*-CRISPRi has clear advantages over conventional shRNA/siRNA approaches. A siRNA approach for *Cacna1h* in mouse embryonic stem cells reduced *Cacna1h* expression levels to approximately 40% but also caused a non-specific decrease in *Cacna1g* mRNA expression levels (Rodríguez-Gómez et al., 2012). By interfering directly with gene promoters, CRISPRa/i modifies corresponding transcript abundance in a way that strongly recapitulates physiological promoter regulation – compared to the above mentioned molecular manipulations, which typically target one specific mRNA variant only. In contrast, CRISPRa/i leads to abundance changes of the respective RNA, which will then be subjected to alternative splicing. Thereby, the abundance

of the full complement of alternatively spliced variants will be increased.

The fact that we did not observe any alterations in the mRNA expression levels of the calcium channel family members *Cacna1g*, *Cacn1i,* and *Cacna1e* clearly indicates that our newly developed *Cacna1h*-CRISPRa/i toolbox is highly specific for *Cacna1h* modulation. Importantly, since the catalytic inactive Cas9 (dCas9) used in our system does not cleave the DNA, the possible off-target effects are more likely to be less deleterious than using the conventional Cas9 to induce a genetic knock-out (Colasante et al., 2020). Compared to genetic knock-out approaches, the *Cacna1h*-CRISPRa/i toolbox, which is based on viral-transduction, allows to decrease *Cacna1h* expression in selected neuron types, by putting dCas expression under the control of cell type specific promoters, in localized brain regions and under temporal control, without time consuming breeding of animals.

Our Tet-On C*acna1h*-CRISPR toolbox system might open new roads for investigating the role of *Cacna1h* in several channelopathies in more detail. Our present study has some limitations. Firstly, we did not test the present CRISPRa/i systems parallel to cell culture in an *in vivo* approach. However, AAV-constructs acting properly in cultured neurons have been successfully translated into *in vivo* applications (Van Loo et al., 2012, 2015). Secondly, we could not scrutinize the effects of CRISPRa/i on a functional level such as by T-type Ca^{2+}-current density or neuronal discharge analyses. Although neuronal cultures constitute a well-known system for studying electrophysiological properties, measuring calcium currents is challenging, especially after modulation of the system. However, all of our previous studies indicate that cellular changes of $Ca_V3.2$ mRNA expression are reflected on the protein level and by changes of current densities and neuronal discharge behavior (Su et al., 2002; Becker et al., 2008; Van Loo et al., 2015).

Also in the context of mutational/genetic ion channelopathies, the potential of inducible *Cacna1h*-CRISPR approaches are immense. For example, in the Genetic Absence Epilepsy Rat from Strasburg (GAERS) a mutation in C*acna1h* has been described, which augments the expression of $Ca_v3.2$ at the cell surface and increases calcium influx (Proft et al., 2017). Here, the *Cacna1h*-CRISPRa could be used as a gain-of-function approach to mimic the enhanced expression seen in GEARS. In addition, a transient inhibition of *Cacna1h via* the Tet-on inducible *cacna1h*-CRISPRi system in the GAERS rats at different stages during development could also reveal potentially interesting time windows for *Cacna1h*-associated channelopathies.

Taken together, our here described *Cacna1h*-CRISPRa/i modular approach could thus be used to model transient gain-of-function or loss-of-function effects in the *Cacna1h* gene and to study $Ca_V3.2$ channelopathies in more detail *in vivo*.

DATA AVAILABILITY STATEMENT

The original contributions presented in the study are included in the article/**Supplementary Material**, further inquiries can be directed to the corresponding author.

ETHICS STATEMENT

The animal study was reviewed and approved by the LANUV Recklinghausen, Leibnizstr. 10, 45659 Recklinghausen.

AUTHOR CONTRIBUTIONS

DT, SS, AB, and KL conceived and planned the study. DT and AT carried out the molecular and cellular experiments. HS, TO, and SS contributed to the study design and analysis. DT wrote the initial draft. AB, SS, and KL contributed to the review and editing. All authors contributed to the article and approved the submitted version.

FUNDING

Our work was supported by the Deutsche Forschungsgemeinschaft (SFB 1089 to AB, SS, and KL, FOR 2715 to AB and HS, SCHO 820/7-2; SCHO 820/5-2; SCHO 820/6-1; SCHO 820/4-1; SCHO 820 5-2 to SS) and BONFOR. AT was supported by the Humboldt Foundation.

ACKNOWLEDGMENTS

We thank Sabine Optiz for excellent technical assistance.

SUPPLEMENTARY MATERIAL

The Supplementary Material for this article can be found online at: https://www.frontiersin.org/articles/10.3389/fnmol.2021.667143/full#supplementary-material

REFERENCES

Becker, A. J., Pitsch, J., Sochivko, D., Opitz, T., Staniek, M., Chen, C. C., et al. (2008). Transcriptional upregulation of Cav3.2 mediates epileptogenesis in the pilocarpine model of epilepsy. *J. Neurosci.* 28, 13341–13353. doi: 10.1523/JNEUROSCI.1421-08.2008

Biermann, B., Sokoll, S., Klueva, J., Missler, M., Wiegert, J. S., Sibarita, J. B., et al. (2014). Imaging of molecular surface dynamics in brain slices using single-particle tracking. *Nat. Commun.* 5:3024. doi: 10.1038/ncomms4024

Cannon, S. C. (2007). Physiologic Principles Underlying Ion Channelopathies. *Neurotherapeutics* 4, 174–183. doi: 10.1016/j.nurt.2007.01.015

Chavez, A., Scheiman, J., Vora, S., Pruitt, B. W., Tuttle, M., Iyer, E. P. R., et al. (2015). Highly efficient Cas9-mediated transcriptional programming. *Nat. Methods* 12, 326–328. doi: 10.1038/nmeth.3312

Chen, J., Sochivko, D., Beck, H., Marechal, D., Wiestler, O. D., and Becker, A. J. (2001). Activity-induced expression of common reference genes in individual CNS neurons. *Lab. Investig.* 81, 913–916. doi: 10.1038/labinvest.3780300

Chhipa, R. R., Fan, Q., Anderson, J., Muraleedharan, R., Huang, Y., Ciraolo, G., et al. (2018). AMP kinase promotes glioblastoma bioenergetics and tumour growth. *Nat. Cell. Biol.* 20, 823–835. doi: 10.1038/s41556-018-0126-z

Cloud-Based Informatics Platform for Life Sciences R&D | Benchling (2021). Available online at: https://www.benchling.com/ [Accessed February 10, 2021].

Colasante, G., Lignani, G., Brusco, S., Di Berardino, C., Carpenter, J., Giannelli, S., et al. (2019). dCas9-Based Scn1a Gene Activation Restores Inhibitory Interneuron Excitability and Attenuates Seizures in Dravet Syndrome Mice. *Mol. Ther.* 28, 235–253. doi: 10.1016/j.ymthe.2019.08.018

Colasante, G., Qiu, Y., Massimino, L., Di Berardino, C., Cornford, J. H., Snowball, A., et al. (2020). In vivo CRISPRa decreases seizures and rescues cognitive deficits in a rodent model of epilepsy. *Brain* 143, 891–905. doi: 10.1093/brain/awaa045

Gilbert, L. A., Larson, M. H., Morsut, L., Liu, Z., Brar, G. A., Torres, S. E., et al. (2013). CRISPR-mediated modular RNA-guided regulation of transcription in eukaryotes. *Cell* 154, 442–451. doi: 10.1016/j.cell.2013.06.044

Heeringa, S. F., Möller, C. C., Du, J., Yue, L., Hinkes, B., Chernin, G., et al. (2009). A novel TRPC6 mutation that causes childhood FSGS. *PLoS One* 4:e7771. doi: 10.1371/journal.pone.0007771

Hutchings, C. J., Colussi, P., and Clark, T. G. (2019). Ion channels as therapeutic antibody targets. *MABS* 11, 265–296. doi: 10.1080/19420862.2018.1548232

Kampmann, M. (2018). CRISPRi and CRISPRa Screens in Mammalian Cells for Precision Biology and Medicine. *ACS Chem. Biol.* 13, 406–416. doi: 10.1021/acschembio.7b00657

Khosravani, H., Altier, C., Simms, B., Hamming, K. S., Snutch, T. P., Mezeyova, J., et al. (2004). Gating Effects of Mutations in the Cav3.2 T-type Calcium Channel Associated with Childhood Absence Epilepsy. *J. Biol. Chem.* 279, 9681–9684. doi: 10.1074/jbc.C400006200

Khosravani, H., Bladen, C., Parker, D. B., Snutch, T. P., McRory, J. E., and Zamponi, G. W. (2005). Effects of Cav3.2 channel mutations linked to idiopathic generalized epilepsy. *Ann. Neurol.* 57, 745–749. doi: 10.1002/ana.20458

Kügler, S., Kilic, E., and Bähr, M. (2003). Human synapsin 1 gene promoter confers highly neuron-specific long-term transgene expression from an adenoviral vector in the adult rat brain depending on the transduced area. *Gene. Ther.* 10, 337–347. doi: 10.1038/sj.gt.3301905

Mizuno, H., Luo, W., Tarusawa, E., Saito, Y. M., Sato, T., Yoshimura, Y., et al. (2014). NMDAR-regulated dynamics of layer 4 neuronal dendrites during thalamocortical reorganization in neonates. *Neuron* 82, 365–379. doi: 10.1016/j.neuron.2014.02.026

Powell, K. L., Cain, S. M., Ng, C., Sirdesai, S., David, L. S., Kyi, M., et al. (2009). A Cav3.2 T-type calcium channel point mutation has splice-variant-specific effects on function and segregates with seizure expression in a polygenic rat model of absence epilepsy. *J. Neurosci.* 29, 371–380. doi: 10.1523/JNEUROSCI.5295-08.2009

Proft, J., Rzhepetskyy, Y., Lazniewska, J., Zhang, F. X., Cain, S. M., Snutch, T. P., et al. (2017). The Cacna1h mutation in the GAERS model of absence epilepsy enhances T-type Ca2+ currents by altering calnexin-dependent trafficking of Cav3.2 channels. *Sci. Rep.* 7:11513. doi: 10.1038/s41598-017-11591-5

Ran, F. A., Hsu, P. D., Wright, J., Agarwala, V., Scott, D. A., and Zhang, F. (2013). Genome engineering using the CRISPR-Cas9 system. *Nat. Protoc.* 8, 2281–2308. doi: 10.1038/nprot.2013.143

Rodríguez-Gómez, J. A., Levitsky, K. L., and López-Barneo, J. (2012). T-type Ca 2+ channels in mouse embryonic stem cells: modulation during cell cycle and contribution to self-renewal. *Am. J. Physiol.* 302, C494–C504. doi: 10.1152/ajpcell.00267.2011

Ryan, D. P., Dias da Silva, M. R., Wah Soong, T., Fontaine, B., Donaldson, M. R., Kung, A. W. C., et al. (2010). Mutations in a potassium channel (Kir2.6) causes susceptibility to thyrotoxic hypokalemic periodic paralysis. *Cell* 140, 88–98. doi: 10.1016/j.cell.2009.12.024

Rzhepetskyy, Y., Lazniewska, J., Blesneac, I., Pamphlett, R., and Weiss, N. (2016). CACNA1H missense mutations associated with amyotrophic lateral sclerosis alter Cav3.2 T-type calcium channel activity and reticular thalamic neuron firing. *Channels* 10, 466–477. doi: 10.1080/19336950.2016.1204497

Savell, K. E., Bach, S. V., Zipperly, M. E., Revanna, J. S., Goska, N. A., Tuscher, J. J., et al. (2019). A neuron-optimized CRISPR/dCas9 activation system for robust and specific gene regulation. *Eneuro* 6, ENEURO.0495–18.2019. doi: 10.1523/ENEURO.0495-18.2019

Souza, I. A., Gandini, M. A., Wan, M. M., and Zamponi, G. W. (2016). Two heterozygous Cav3.2 channel mutations in a pediatric chronic pain patient: recording condition-dependent biophysical effects. *Pflugers Arch. Eur. J. Physiol.* 468, 635–642. doi: 10.1007/s00424-015-1776-3

Souza, I. A., Gandini, M. A., Zhang, F. X., Mitchell, W. G., Matsumoto, J., Lerner, J., et al. (2019). Pathogenic Cav3.2 channel mutation in a child with primary generalized epilepsy. *Mol. Brain* 12:86. doi: 10.1186/s13041-019-0509-5

Splawski, I., Yoo, D. S., Stotz, S. C., Cherry, A., Clapham, D. E., and Keating, M. T. (2006). CACNA1H mutations in autism spectrum disorders. *J. Biol. Chem.* 281, 22085–22091. doi: 10.1074/jbc.M603316200

Su, H., Sochivko, D., Becker, A., Chen, J., Jiang, Y., Yaari, Y., et al. (2002). Upregulation of a T-Type Ca2+ Channel Causes a Long-Lasting Modification of Neuronal Firing Mode after Status Epilepticus. *J. Neurosci.* 22, 3645–3655. doi: 10.1523/jneurosci.22-09-03645.2002

Thakore, P. I., D'Ippolito, A. M., Song, L., Safi, A., Shivakumar, N. K., Kabadi, A. M., et al. (2015). Highly specific epigenome editing by CRISPR-Cas9 repressors for silencing of distal regulatory elements. *Nat. Methods* 12, 1143–1149. doi: 10.1038/nmeth.3630

Van Loo, K. M. J., Rummel, C. K., Pitsch, J., Müller, J. A., Bikbaev, A. F., Martinez-Chavez, E., et al. (2019). Calcium channel subunit α2σ4 is regulated by early growth response 1 and facilitates epileptogenesis. *J. Neurosci.* 39, 3175–3187. doi: 10.1523/JNEUROSCI.1731-18.2019

Van Loo, K. M. J., Schaub, C., Pernhorst, K., Yaari, Y., Beck, H., Schoch, S., et al. (2012). Transcriptional regulation of T-type calcium channel CaV3.2: bi-directionality by early growth response 1 (Egr1) and repressor element 1 (RE-1) protein -silencing transcription factor (REST). *J. Biol. Chem.* 287, 15489–15501. doi: 10.1074/jbc.M111.310763

Van Loo, K. M. J., Schaub, C., Pitsch, J., Kulbida, R., Opitz, T., Ekstein, D., et al. (2015). Zinc regulates a key transcriptional pathway for epileptogenesis via metal-regulatory transcription factor 1. *Nat. Commun.* 6, 1–12. doi: 10.1038/ncomms9688

Wang, Q., Curran, M. E., Splawski, I., Burn, T. C., Millholland, J. M., VanRaay, T. J., et al. (1996). Positional cloning of a novel potassium channel gene: kVLQT1 mutations cause cardiac arrhythmias. *Nat. Genet.* 12, 17–23. doi: 10.1038/ng0196-17

Woitecki, A. M. H., Müller, J. A., van Loo, K. M. J., Sowade, R. F., Becker, A. J., and Schoch, S. (2016). Identification of synaptotagmin 10 as effector of NPAS4-mediated protection from excitotoxic neurodegeneration. *J. Neurosci.* 36, 2561–2570. doi: 10.1523/JNEUROSCI.2027-15.2016

Yeo, N. C., Chavez, A., Lance-Byrne, A., Chan, Y., Menn, D., Milanova, D., et al. (2018). An enhanced CRISPR repressor for targeted mammalian gene regulation. *Nat. Methods* 15, 611–616. doi: 10.1038/s41592-018-0048-5

Zhang, J., Chen, L., Zhang, J., and Wang, Y. (2019). Drug Inducible CRISPR/Cas Systems. *Comput. Struct. Biotechnol. J.* 17, 1171–1177. doi: 10.1016/j.csbj.2019.07.015

Zhong, X., Liu, J. R., Kyle, J. W., Hanck, D. A., and Agnew, W. S. (2006). A profile of alternative RNA splicing and transcript variation of CACNA1H, a human T-channel gene candidate for idiopathic generalized epilepsies. *Hum. Mol. Genet.* 15, 1497–1512. doi: 10.1093/hmg/ddl068

Conflict of Interest: The authors declare that the research was conducted in the absence of any commercial or financial relationships that could be construed as a potential conflict of interest.

Publisher's Note: All claims expressed in this article are solely those of the authors and do not necessarily represent those of their affiliated organizations, or those of the publisher, the editors and the reviewers. Any product that may be evaluated in this article, or claim that may be made by its manufacturer, is not guaranteed or endorsed by the publisher.